Industrial Crops & Products 222 (2024) 119629

Contents lists available at ScienceDirect

Industrial Crops & Products

journal homepage: www.elsevier.com/locate/indcrop

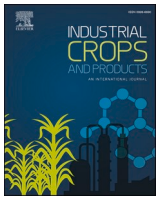

Waste management of straw to manufacture biochar: An alternative reinforcing filler for natural rubber biocomposites

Justyna Miedzianowska-Masłowska *, Marcin Masłowski, Maciej Delekta, Krzysztof Strzelec

Institute of Polymer and Dye Technology, Lodz University of Technology, Stefanowskiego 16, Lodz 90-537, Poland

ARTICLE INFO

Keywords:
Biochar
Filler
Polymer composite
Rubber
Carbon black

ABSTRACT

To achieve climate neutrality, alternative processes and materials should be proposed to replace those currently in use, which excessively burden the environment. Fossil fuels are non-renewable, and their resources are slowly being depleted, leading to increased prices.

The aim of this work was to determine the potential of using agro-industrial residues in the form of oat straw for the production of biochar and its utilization as a filler in natural rubber biocomposites. The process of pyrolysis of plant material was used to obtain biochar with a high carbon content and a characteristic structure, which can affect selected rubber properties. The influence of the applied temperature of the pyrolysis process on the properties of the filler was determined. In this work, analysis techniques were used to enable the evaluation of both filler activity and specific properties of the final vulcanizates. The course of straw pyrolysis process, the carbon content in the fillers, and the size distribution of the bio-additive were examined. The structural, morphological, dispersion, processing, and functional properties of the compositions were examined. The reference in assessing the impact of the produced bio-additive on the properties of the product were composites filled with a commercial carbon black.

The conducted research proved that the pyrolysis of straw at a temperature of 600 °C was as effective as that carried out at a higher temperature, with comparable weight loss for both samples. The increase in torque was the highest in the case of biochar samples (torque gain 4,4–6,5 dNm), indicating greater intensity of the cross-linking process after the use of this type of additive. This was also confirmed by differential scanning calorimetry. Moreover, the obtained biocomposites were characterized by much higher strength parameters (tensile strength 18,3–21,3 MPa) than conventional composites. Unfortunately, vulcanizates containing biochar as a filler exhibited poor resistance to thermo-oxidative aging (aging factor 0,24–0,54).

1. Introduction

Carbon black (CB) is a commonly used material in science and technology. It is most often used as a reinforcing phase in the preparation of elastomeric composites, such as tires, conveyor belts, air springs, sealers, and insulator devices (Fan et al., 2020). Unfortunately, the production process of CB is characterized by a large carbon footprint. This material is derived from fossil fuels through an incomplete combustion reaction, typically carried out at 1400 °C (Wang et al., 2020). Depending on the specific material requirements, various morphological varieties of carbon black that meet these criteria can be used (Kumar et al., 2008). The main parameters describing the properties of carbon fillers are particle size, morphology, specific surface area, which affect their activity in the polymer medium (Ulfah et al., 2015). Since this raw material is obtained from fossil sources, not from the atmosphere, and part of the carbon is oxidized, this process generates significant amounts of greenhouse gases.

An alternative to renewable carbon black is the use of biochar (BC), of which various types have been used for thousands of years, with wood being the most common. The main components of bio-additives obtained from raw materials of plant origin are cellulose, hemicellulose, and lignin. As the different forms of organic matter are present around the world, the exact proportion of these constituents depend on the method of biochar formation (Kumar et al., 2008): hydrothermal liquefaction, pyrolysis and gasification (Bartoli et al., 2022). Nowadays, pyrolysis is the main method for biochar production, which involves the thermal degradation of organic material in an inert atmosphere (Al-Rumaihi et al., 2022; Gabhane et al., 2020). Products such as

* Corresponding author.
E-mail address: justyna.miedzianowska@p.lodz.pl (J. Miedzianowska-Masłowska).

https://doi.org/10.1016/j.indcrop.2024.119629
Received 20 May 2024; Received in revised form 28 August 2024; Accepted 7 September 2024
Available online 9 September 2024

bio-char, bio-oil and bio-gas are the main goods produced in this process. Although straightforward, numerous factors play crucial roles in the final properties of obtained solids as well as the proportion between products. The final characteristics may depend on the process conditions, which include: time, temperature and temperature rise rate, gas flow, mixing, and additive presence (Sarkar and Wang, 2020).

Traditionally, biochar was utilized as an energy source. However, recently more and more studies are being published about advanced technological applications of such materials. Among the applications of biochar, the most important so far is its use as an adsorbent (Garg and Das, 2020) activated carbon (Scapin et al., 2020), soil amender (Guo et al., 2020), or catalysts support (Chen et al., 2020). Currently, it is used in industries such as water treatment, agriculture, construction, or composite material production (Nagarajan et al., 2016). There is increasing interest in tailoring properties through the pyrolysis process conditions. Biochar, as a filler, has already been applied in some polymers. It is obtained from various sources for instance, soy husks and coffee (Quosai et al., 2018). Ramaswamy et al. used biochar obtained from pear and onion as a filler for epoxy resin composites (Ramaswamy et al., 2022). Numerous other polymer matrixes in which this novel material has been utilized include polyamides, ethyl polyethylene terephthalate, polypropylene, polycarbonates, polybutylene terephthalate, and others (Gupta et al., 2022). Generally, biochar can be used as a filler material in a wide range of thermosetting, thermoplastic and ceramic polymer composites to improve their mechanical, thermal and electrical properties (Aboughaly et al., 2023). Considering their properties and the benefits of biochar application, such materials can have potential applications in various industries. Among them, we can mention packaging, automotive, aerospace, mining and construction (Tengku Yasim-Anuar et al., 2022). However, there are still limited published studies on the implementation of biochar into polymeric materials. This may be due to the lack of knowledge about the potential effect of biochar on polymers. An equally interesting issue is to learn about the influence of biochar on the characteristics of the vulcanization process of elastomer composites, which has not been described in the literature so far. Vulcanization is a technological process aimed at transforming rubber or a plastic rubber mixture into elastic rubber, which is a material with appropriate utility properties (Maciejewska and Sowińska-Baranowska, 2022). The effect of vulcanization is the connection of elastomer chains through cross-linked chemical bonds and the creation of a three-dimensional spatial network (Ikeda, 2014).

Cereal straw is gaining a lot of interest as a generally accessible raw material that can be used to produce environmentally friendly consumer goods through appropriately selected processing or modification. In European countries, it is considered one of the most interesting and requiring management raw materials derived from agricultural waste with high application potential for the biochemical industry (Björnsson and Prade, 2021). According to Kalak (Kalak, 2023) approximately 360 million tons of biomass in the form of straw are currently used worldwide. Its uses include processing in the pulp and paper industry as a source of fibers; used in the furniture industry for the production of particleboard; construction - insulating materials; agriculture as animal feed and bedding; energy sector - energy recovery during incineration (Masłowski et al., 2017). Moreover, it is estimated that in Europe approximately 10 million tons of crop residues could constitute a valuable source of material in modern bio-industries without negative impacting eco-processes, such as soil fertilization or protection of soil organic matter.The availability, low cost, and renewable and natural character of straw make it an excellent resource for obtaining biochar.

The leading company in the automotive industry, Bridgestone, has announced its pro-ecological mission, which assumes that its tires will be completely made from eco-friendly materials. Another brand, Michelin, has a very similar long-term vision, aiming of 100 % of its goods to be manufactured from bio-inspired and recycled materials by 2050 (Greenough et al., 2021). The application of bio-sources fillers could contribute to further decreasing the dependence of different techniques and processes on fossil fuels.

Straw management for the production of biochar used as a bio-additive in the natural rubber composition is a research novelty. Numerous studies on biochar usually concern the characteristics of the product obtained at various times (Mohd Hasan et al., 2019) and temperature conditions (Zhao et al., 2017). There is more and more information in the latest news about the use of biochar, as already mentioned, also as an additive in polymer materials. The application of biochar as a functional filler in thermoplastic matrices such as HPDE (Q. Zhang et al., 2020), PLA (Anerao et al., 2023) and others (Haleem et al., 2022) is known. Much less attention is paid to elastomeric compounds, which also play a significant role in the industry. Recently, however, there have been literature reports on the characteristics of biochar from the point of view of its implementation as reinforcement in elastomers (Abd El-Aziz et al., 2022; Bardha et al., 2024). Peterson et al. conducted research in which biochar was mixed with carbon black and use in styrene–butadiene rubber (Peterson et al., 2016). A similar research problem was also explored by Abd et al. (Abd El-Aziz et al., 2022). Other studies attempted to reduce biochar particles with nanosilica and determine its effect on the properties of polymer materials (Peterson and Kim, 2020). These studies focused mainly on strength tests of rubber composites. In research on the application of biochar to an elastomeric matrix, an attempt was made to test the effect of bamboo-biochar loading on the damping and acoustical characteristics of natural rubber vulcanizates (Sunali et al., 2022). When reviewing the literature on the application of biochar in elastomeric composites, the vast majority concerns vulcanizates based on synthetic rubbers. The primary goal of the work is to identify cereal straw as a waste source of matter for obtaining biochar serving as an alternative and functional filler for rubber composites.

Based on the outlined research objectives and considerations, the authors hypothesize that the utilization of straw biochar as a bio-additive in natural rubber composites will yield green materials with enhanced structural and performance characteristics. It is worth noting that the work presents the influence of biochar on the aging processes of NR vulcanizates; this aspect has not been reported so far in open literature on the use of biochar as a filler in polymer composites. Moreover, the main source of biochar is various types of wood (Ayadi et al., 2020). Other waste raw materials, such as straw, are much less analyzed in terms of the possibility of obtaining biochar and its application in elastomeric composites. This paper presents studies on the effect of the temperature of straw conversion in the process of pyrolysis to biochar on its characteristics, as well as on the subsequent properties of rubber vulcanizates filled with the obtained biocarbon fillers. Moreover, the results were compared with the commercial filler, which is N550 carbon black.

2. Materials and methods

2.1. Materials

Natural rubber (NR) RSS I (Torimex-Chemicals, Poland) was used as the polymer matrix.

Sulfur (S), zinc oxide (ZnO), stearic acid (SA) 2-mercaptobenzothiazole (MBT) (all delivered by Sigma–Aldrich, USA) were applied as a curing system.

Fillers:

- Carbon black (CB), N550 (Konimpex, Poland);
- Biochars (BC).

Oat straw (*Avena sativa L.*) was collected from local farmers in Poland. After initial drying at 70 °C for 48 h, the material was cut down into smaller pieces and milled with planetary ball mill (time: 1 hour, rotation speed: 300 rpm). After this, the material was further dried for an additional 24 hours.

2.1.1. Preparation of biochar

To obtain biochar, ground straw (25 g) was placed in a specially prepared crucible with a supply of inert gas (nitrogen). Additionally, the vessel was equipped with an outlet enabling the removal of gaseous and condensed biomass transformation products, which were not subjected to further analysis. The vessel was placed in a muffle furnace with ports enabling the inlet and outlet of gases. High-temperature treatment was performed at temperatures of 600 °C (BC1) and 900 °C (BC2) with a heating rate of approx. 10 °C/min. After reaching the set temperature, there was a stabilization period of 2 h. During the process, the nitrogen flow rate was 2 l/h. The residue was then left in the vessel to cool for 2 h during which the nitrogen flow was also maintained. The obtained solid fraction - biochar constituted material for further research. Then the material was weighed to calculate the efficiency of the pyrolysis process.

2.2. Methods

2.2.1. Biochar yield

Biochar yield (BCY) was calculated using the following Eq. (1)

$$BCY = \frac{m_1}{m_2} \times 100\% \quad (1)$$

m_1 - weight of sample of biomass before pyrolysis [g], m_2 - weight of biochar [g].

2.2.2. Thermogravimetric analysis

A thermogravimetric analyzer (Mettler Toledo, Greifensee, Switzerland) was used to analyze the thermal properties of the obtained filler materials. Samples (approx. 10 mg) were heated (10 °C/min) from room temperature to 700 °C under an argon atmosphere (flow 55 mL/min) and then in the range 700–800 °C with air (55 mL/min).

2.2.3. Granulometry

A vibrating table (AS200 Control, Retsch GmbH, Haan, Germany) and sieves with mesh sizes: 4.0, 2.0, 1.0, 0.5, 0.25 and 0.125 mm were used for sieve analysis. The amount of filler used for the test was invariably 20 g. Sieving was carried out for 3 minutes with a vibration amplitude of 1.5 mm. The obtained fractions were weighed on Radwag analytical scales. The size fraction was determined by the total sum of all fractions.

2.2.4. Elementary analysis

Elemental analysis of the tested carbon fillers was performed using the NA2500 apparatus (CE INSTRUMENTS, Wigan, United Kingdom), which uses the method of rapid, complete combustion of samples in oxygen. The analysis methodology was prepared by the manufacturer according to the ISO 16948 standard. Combustion takes place in a column heated to 1000 °C. After combustion, the resulting gases are analyzed by gas chromatography. By burning several samples of known composition, the mass of the analyzed elements (C, H, N, S) depends on the area under the peak in the chromatogram. To obtain the highest possible accuracy, the standard should be selected appropriately so that the content (mass fraction) of the element in the standard is similar to its content in the analyzed sample. The ATROPINE standard was used to determine the carbon content (C% = 70.56). The correctness of the determination was checked on this standard and 2,5-(Bis(5-tert-butyl-2-benzo-oxazol-2-yl)thlophene (BBOT C% = 72.54) and Methionine (C 40.25 %). All standards are certified by Elemental Microanalysis.

2.2.5. SEM analysis

Scanning electron microscope (SEM), specifically LEO 1530 Gemini (Zeiss/LEO, Germany) equipped with the energy dispersive spectrometer (EDS) was employed to determine the shape, size and morphology of carbon filler samples. Rubber composites (cross-sectional morphology) were also tested. The EDS method was used to perform an elemental analysis of micro-areas of mineralized biochar samples. The measurements required preliminary processing by applying a carbon layer with the Cressington 208 HR system.

2.2.6. Preparation of Rubber mixes

A laboratory micromixer (Brabender, Duisburg, Germany) was used to mix the rubber ingredients (without a curing system). The rotational speed was 40 rpm, in turn, the temperature was 50 °C. Compounds were mixed for 8 min, where the first 4 mins were used to plasticize rubber and a further 4 min to homogenize rubber with a filler. Next, the BRIDGE laboratory two-roll mill was enrolled to mix a sulphur cross-linking system (ZnO 5 phr, S 2 phr, MBT 2 phr, SA 1 phr) to the composition. The length and the diameter of the rollers were equal to 450 mm and 200 mm respectively, the gap was set to 1.5–3 mm, the rotation speed of the first roller was 16 rpm, friction was 1–1,2 and the average temperature was set to around 30 °C. The time of mixing for one sample was 10 minutes. The exact composition of the rubber composites produced is illustrated in Table 1.

2.2.7. Rheometric properties

The following study was performed with the utilization of MDR rheometer (Alpha Technologies, Hudson, USA) according to ISO 6502 standard. The temperature was set to 160 °C. Minimum and maximum torque (M_{min}, M_{max} respectively), and optimal vulcanization time (t_{90}) were measured and determined. The torque increase for rubber mixtures was determined based on Eq. (2):

$$\Delta M = M_{max} - M_{min} \quad (2)$$

2.2.8. Composites preparation

The vulcanization process was performed for 10 minutes (temperature: 160 °C, pressure: 15 MPa). The rubber mixtures were placed in steel molds and heated in a hydraulic press. In order to prevent the material from sticking to the surface of the molds, Teflon foil was used. As a result of vulcanization, rectangular samples with dimensions of 100 × 80 × 1 mm were obtained. The rubber composites were used for further tests of their properties.

2.2.9. Cross-linking density

Rubber samples (approx. 20–40 mg.) placed in a toluene solvent undergo a swelling process (48 h). After this period, the swollen samples were weighed (m_{sw}) and then dried at 50 °C in a thermocirculation dryer for 24 hours. Then the mass was measured again (m_s). The sample weight increase can be coordinated with the cross-linking density based on the Flory-Rehner Eq. (3).

$$\gamma_e = \frac{\ln(1 - V_r) + V_r + \mu V_r^2}{V_0\left(V_r^{\frac{1}{3}} - \frac{V_r}{2}\right)} \quad (3)$$

νe-the cross-linking density (mol/cm^3)

V_0-the molar volume of solvent (toluene:106.7 cm^3/mol),

μ—for the interaction of natural rubber—toluene at 25 °C, the Huggins parameter (Eq. (4)) is equal to:

$$\mu = 0.478 + 0.228 \times V_r \quad (4)$$

Vr - the volume fraction of elastomer in the swollen gel (Eq. (5)).

$$V_r = \frac{1}{1 + Q_w \frac{\rho_r}{\rho_s}} \quad (5)$$

ρ_r - density of rubber (0.99 g/cm^3), ρ_s - density of solvent (0.86 g/cm^3), Q_w - the weight of equilibrium swelling (Eq. (6)):

$$Q_w = \left(\frac{m_{sw} - m_s}{m_s}\right) \times \left(\frac{100 + x}{100}\right) \quad (6)$$

Table 1
Formulation of polymer mixtures.

Sample	NR [phr]	CB [phr]	BC1 [phr]	BC2 [phr]	ZnO [phr]	S [phr]	MBT [phr]	SA [phr]
NR0	100	-	-	-	5	2	2	1
NR_CB_10		10						
NR_CB_20		20						
NR_CB_30		30						
NR_BC1_10		-	10					
NR_BC1_20			20					
NR_BC1_30			30					
NR_BC2_10			-	10				
NR_BC2_20				20				
NR_BC2_30				30				

phr - parts per hundred of rubber.

m_{sw} - the weight of the swollen sample;
m_s - the weight of the dry sample;
100 - the elastomer content in the sample;
x - the filler content in the sample.

The average values (based on 4 samples) were presented along with their standard errors, and the data were subsequently analyzed using a one-way ANOVA. The statistical analysis demonstrated that the vulcanizates containing different carbon additives exhibited a statistically significant difference in γe ($p < 0.05$). The cross-linking density of the samples was determined both for the composites before aging and after the simulated thermo-oxidative aging process.

2.2.10. Mechanical properties study

A universal testing machine (ZwickRoell, Ulm, Germany) was applied to measure strength parameters such as: tensile strength and elongation at break. The analysis was based on the ISO-37 standard. The samples were shaped into type 3 dumbbells, each measuring 4 mm in width and 1 mm in thickness. The stretching speed was adjusted to 500 mm/min. The study allowed to determine: stress at 300 % elongation (SE_{300}), tensile strength (TS) and elongation at break (EB). The average values were presented alongside their standard errors, and a one-way analysis of variance (ANOVA) was conducted for analysis. The statistical examination revealed a significant difference in mechanical properties among composites with different carbon fillers ($p < 0.05$). The mechanical properties of the samples was determined both for the composites before aging and after the simulated thermo-oxidative aging process.

2.2.11. Thermo-oxidative ageing influence

The assessment of the effects of thermo-oxidative aging on vulcanizates was conducted following the PN-82/C-04216 standard. The vulcanizates were exposed to oxygen at elevated temperatures for 14 days. For this purpose, an FD Binder dryer with hot air circulation was used. The temperature was set to 70 °C. After the simulated aging process of the vulcanizates, mechanical properties and equilibrium swelling were measured. To describe the aging effect, the K parameter was calculated according to Eq. (3) below. This value compares the properties before and after aging (Eq. (7)).

$$K = \frac{TS_{AA} \times EB_{AA}}{TS_{BA} \times EB_{BA}} \quad (7)$$

TS-tensile strength, EB-relative elongation at break, AA is the property measured after ageing and BE before ageing.

2.2.12. Dynamic scanning calorimetry

The glass transition temperature (Tg), and vulcanization enthalpy (ΔH), as well as the initial and final temperatures, were assessed for the prepared biocomposites by differential scanning calorimetry DSC (Mettler Toledo, Switzerland). The measurement was conducted in a surrounding argon atmosphere. The 10 milligrams of rubber samples were chilled to −150 °C and held steady for 5 minutes. Subsequently, the sample was heated gradually at a rate of 10 °C per minute until it reached a temperature of 240 °C. Heat flows were measured, and characteristic points were established through STARe software.

2.2.13. Dynamic-mechanical analysis (Payne effect measurement)

Dynamic mechanical analysis was carried out by the Ares G2 rheometer (TA Instruments, New Castle, DE, USA). A 2 mm thick rubber disk with a diameter of 25 mm was placed in the measuring gap (plate-plate). Shear force (2 N) was applied with a constant temperature (25 °C) and strain frequency (0.1–100 %). Shear deformation was increased with time. Storage and loss modulus (G' and G'') were plotted on a graph as a function of shear deformation amplitude for all tested biocomposites. Eq. (8) was used to calculate the Payne effect.

$$(\Delta G' = G'_{min}(\lim 10^{-1}) - G'_{max}(\infty)) \quad (8)$$

G'_{min} and G'_{max} - values of the loss modulus at the minimal and maximal applied shear strain amplitude.

3. Results and discussion

3.1. Biochar yield and elemental analysis of carbon content

Based on mass measurements before and after the pyrolysis process, its efficiency was determined and presented as a percentage of the residue after high-temperature treatment of plant material. Elemental analysis was also performed, on the basis of which the carbon content in the obtained biochar (BC) and in the reference sample of carbon black (CB) was determined. The results of these analyses are presented in Table 2.

The biomass pyrolysis process leads to the formation of primary products such as bio-char, oils and fuel (Tripathi et al., 2016). Based on the conducted field measurements, thermal treatment contributed to the removal of approximately 75 % of the matter, mainly hydrocarbons, carbon, sulfur and nitrogen oxides, as well as water. A slight decrease in pyrolysis efficiency was noticeable at higher temperatures. This is an effect often observed in studies on the pyrolysis of plant materials for conversion to biochar (TSAI et al., 2007; X. Zhang et al., 2020). The BCY was reduced from 28,4 to 26,0 %, for treatment temperatures of 600 and 900 °C, respectively. This is because at higher temperatures, lignocellulosic components are quickly and comprehensively decomposed, resulting in a reduction in BCY. The obtained results of the efficiency of biochar produced in high-temperature processing of straw biomass

Table 2
Biochar characteristic.

Sample	Process temperature [°C]	BCY [%]	Carbon (C) content [%]
BC1	600	28,4±0,4	72,2
BC2	900	26,0±0,5	75,0
CB	-	-	>95

aligned with those documented in the literature. Selvarajoo et. al obtained similar performance parameters for biochar produced in the rice straw pyrolysis process. In their case, the biochar yield decreased from 29.93 % to 26.67 for temperatures of 500 and 900 °C, respectively (Selvarajoo and Oochit, 2020). Elevated temperatures and prolonged residence durations enhance the transformation of biomass into gas (Bridgwater, 2012).

As confirmed by elemental analysis, high-temperature straw processing resulted in fillers that were a carbon (C)-rich by-product (Table 2), with analysis of the carbon content of the samples showing an increase in the presence of this element in the filler with increasing straw processing temperature. This was caused by the increased release of volatile substances with rising heat treatment temperature (Zhao et al., 2017). A similar effect was observed by other research teams focusing on the characteristics of biochar obtained from plant biomass (Zhao et al., 2017). This could be attributed to the rising temperature causing more extensive cracking of the volatile fractions into low molecular weight liquids and gases, rather than biochar formation (Ronsse et al., 2013). Moreover, an increase in temperature may favor other reactions such as dehydration of hydroxyl groups, as well as thermal decomposition of cellulose and lignin, leading to a rise in the overall char content in the samples (Zhang et al., 2015). At higher temperatures, much more intense gasification reactions of decarburizing steam occur, favoring the transformation of charcoal into a hydrogen-rich gas (Zhao et al., 2017).

3.2. Thermogravimetric analysis of plant material

In order to characterize the pyrolysis process, various research techniques are used, one of the more advanced is Py-GC-MS, which allows for the analysis of chemical components, as well as the study of pyrolysis decomposition products. Another preliminary technique useful for assessing the course of thermal processes occurring with the change of mass, for example during combustion or thermal decomposition of materials, is thermogravimetric analysis (TGA). Table 3 presents the parameters of the TGA test carried out on the oat straw material. The supplementary materials include TG and DTG curves of oat straw samples (Fig S1.). The heating process was carried out in an inert gas atmosphere, corresponding to the conditions prevailing during the preparation of biochar on a larger scale (muffle furnace).

The thermal decomposition of straw took place in several stages, with individual steps distinguished, such as evaporation of moisture, and decomposition of carbohydrates that make up natural fibers: hemicellulose, cellulose, and lignin. The thermogram distinctly illustrates the phases associated with the thermal decomposition of straw materials. The initial mass loss of the straw occurring in the temperature range of 25–120 °C, was related to the removal of water bound in the natural fiber. The moisture content of the straw sample was approximately 6 %. Then, the main stage of pyrolysis took place, i.e. the decomposition of organic substances into carbon, water and other volatile and liquid compounds. Considering the TG curves, the degradation stages between 180 and 700 °C encompassed the thermal decomposition of the basic components of straw (cellulose, hemicellulose and lignin). Among them, hemicellulose is characterized by the lowest thermal stability, and its degradation occurs at temperatures of 200–300 °C (Yang et al., 2007). In contrast, cellulose is characterized by a narrow range of thermal decomposition, which is between 315 and 400 °C (Shahbaz et al., 2022). Due to the fact that the distribution ranges of these two compounds partially overlap, one clear signal is usually observed on the DTG curve. Similar behavior of plant material samples during pyrolysis kinetics studies was also observed by other authors (Grønli et al., 2002; Kim et al., 2012). On the other hand, lignin degradation occurs in a much wider temperature range of 200–700 °C. According to literature sources (Burhenne et al., 2013), due to its structure, which includes unsaturated bonds occurring in alkylbenzene, lignin is very stable and, furthermore, much more difficult to decompose than other components, hence the wider spectrum of thermal decomposition. The maximum rate of weight loss of the straw material sample occurred at 315 °C, i.e.

In the range from 150 to 600 °C, the loss of mass of materials ($\Delta m_{150–600}$) amounted to almost 70 %, while considering the range of 150–900 °C, the loss of mass amounted to over 76 %. The obtained results indicated an intensive process of thermal decomposition of plant material with a significant loss of matter. The remaining solid matter after thermal degradation (R_{900}) for the oat straw sample was about 17 %. Considering the residue at 600 °C R_{600} (23.5 %), this value corresponded to the efficiency of the straw pyrolysis process (Table 2). This proves that the proposed method of heating the material in a crucible with an inert gas provided appropriate conditions for biomass pyrolysis. In the solid residue after analysis, in addition to carbon, inorganic compounds may also be present. The authors' previous studies on the characteristics of plant materials, including straw, showed the presence of calcium, magnesium, and silicon compounds (Masłowski et al., 2021).

Table 3
Thermogravimetric analysis of oat straw samples.

Sample	$\Delta m_{25–150}$ %	$\Delta m_{150–600}$ %	$\Delta m_{150–900}$ %	R_{600} %	R_{900} %
Straw	6,6	69,9	76,2	23,5	17,2

3.3. Particle size analysis

Particle size, dispersion and specific surface area are key parameters influencing the formation of the filler network in the polymer medium. The size of particles impacts the activity of additives, which in turn affects the strengthening effect. Large particles can concentrate stress and result in decreased composite strength, whereas excessively small particles are challenging to disperse and tend to agglomerate. In turn, the interactions inside the filler-filler agglomerate are weaker than the filler-polymer interactions, which usually means that as the size of the agglomerates increases, their ability to inhibit crack propagation decreases. The results below did not refer to the final size of the agglomerates in the polymer matrix, because during processing when adding the filler to the elastomer, shear forces acted on it, which could further reduce their size. On the other hand, in the elastomeric matrix, the additive particles agglomerated and aggregated, very rarely appearing in the form of primary particles. Nevertheless, the granulometric examination allowed us to determine whether there is a need to reduce the particle size by using an additional processing step, such as grinding, before addition to the polymer matrix. Additionally, it provided information about size dispersion. In the case of large dispersion, operations aimed at greater homogenization should be used, for example sieving the material. Fig. 1 shows the results of fraction distribution for fillers obtained at temperatures of 600 °C (B1) and 900 °C (B2).

Analyzing the results, it can be clearly stated that the largest fraction in terms of quantity was the smallest fraction, with a size below 0.045 mm. It is worth noting, however, that the fractions of 0.063 mm and 0.045 mm had very similar percentages. This means that most of the material was so small that it could not be analyzed using this technique. Taking into account the results obtained, it turned out that there was no need to use additional methods to reduce the size of the filler, such as mechanical modification. When comparing fillers obtained at two different temperatures, it should be noted that the lower pyrolysis temperature led to a rise in the content of the additive with fractions of 0.063 mm and 0.045 mm. In contrast, when a temperature of 900 °C was used, a higher percentage of the biofiller consisted of particles with dimensions below 0.045 mm.

3.4. Morphology of samples

To determine the morphology of carbon biofiller samples produced

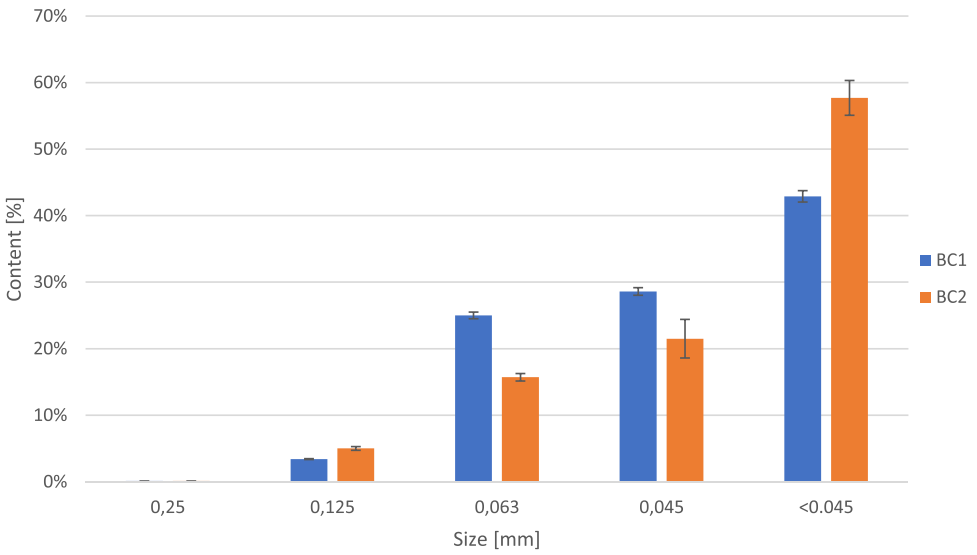

Fig. 1. Sieve analysis of biochar samples.

(a)

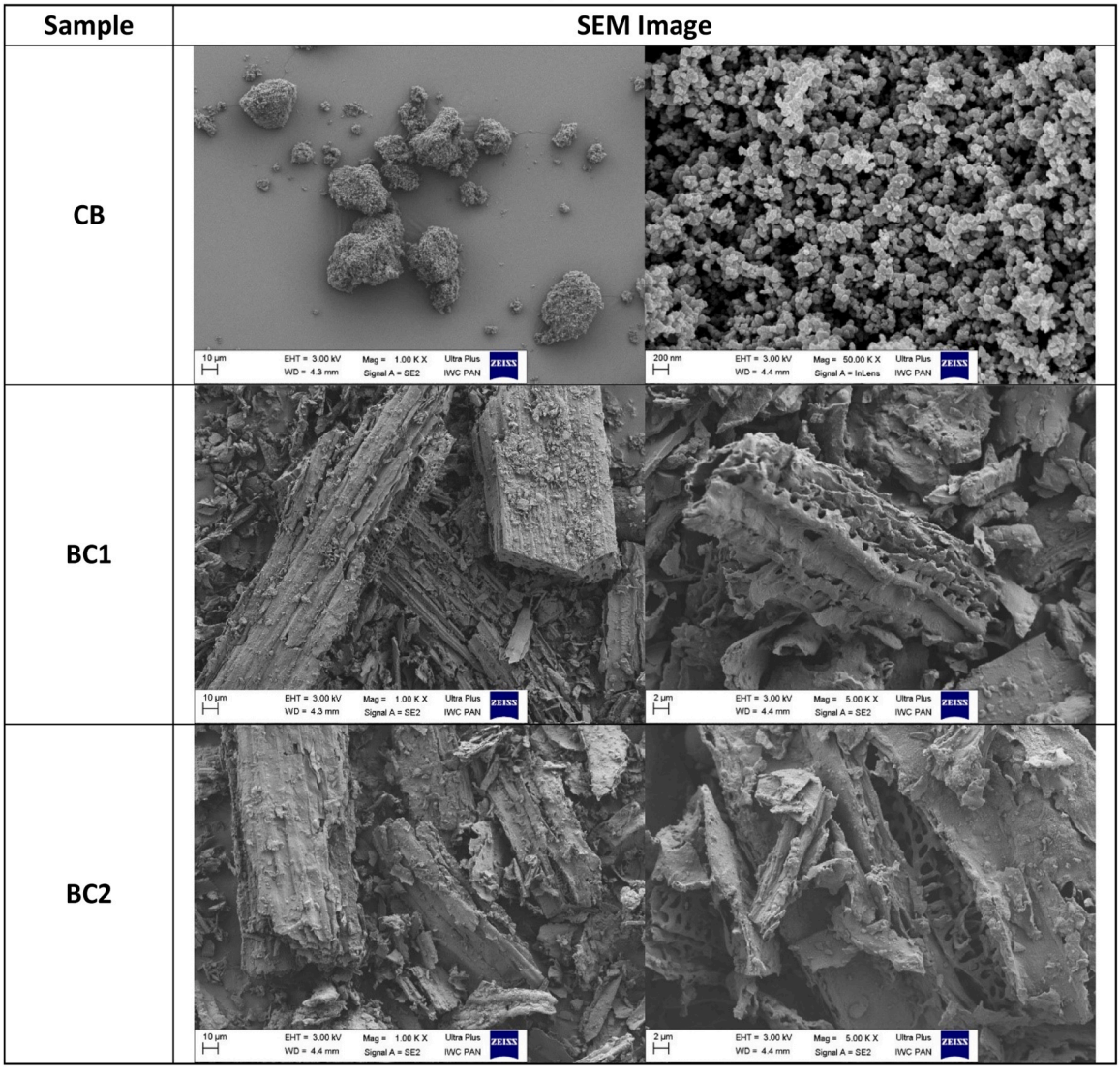

Fig. 2. SEM images of carbon fillers (a) and prepared composites (b).

(b)

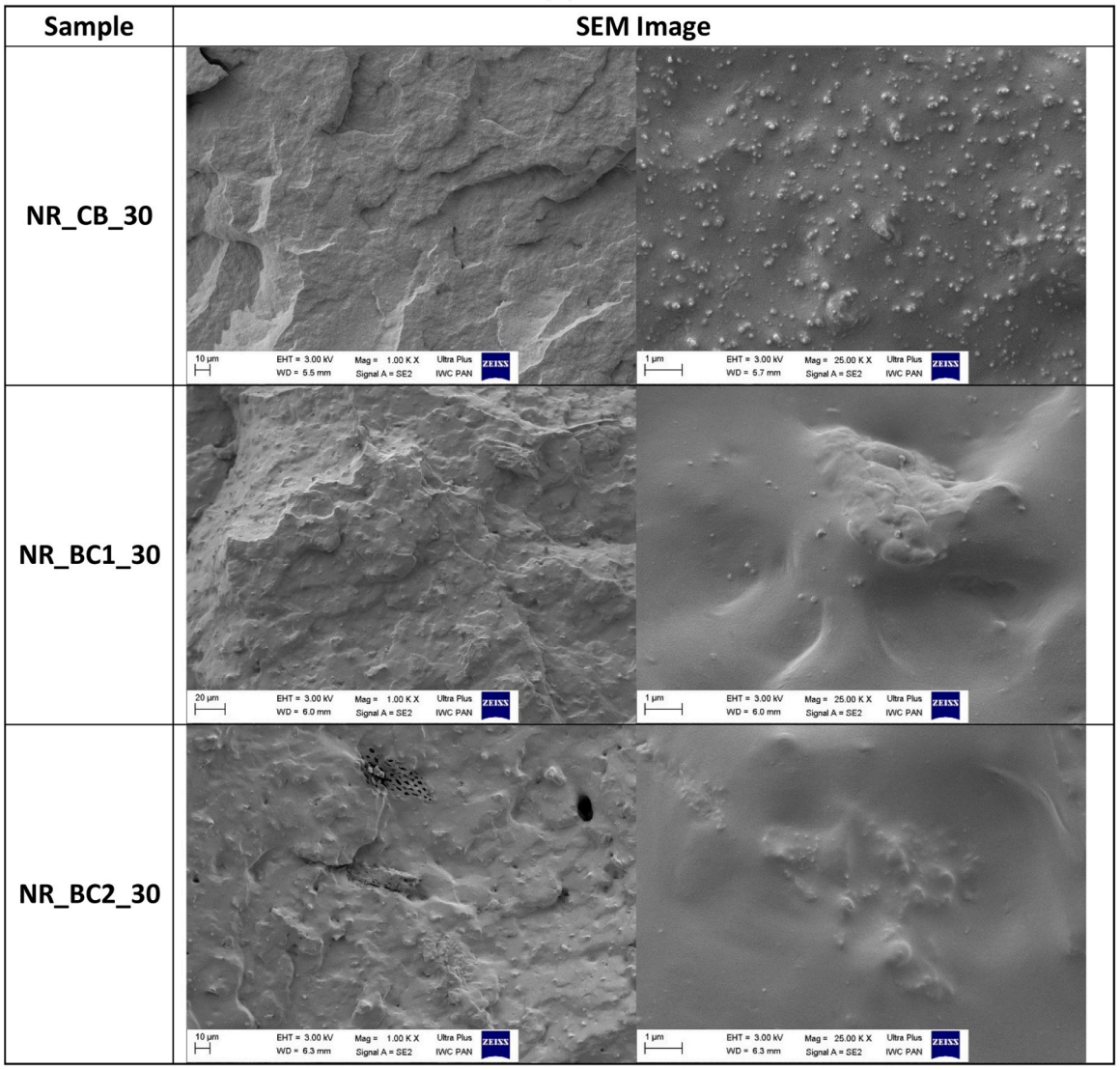

Fig. 2. (*continued*).

during straw pyrolysis, SEM images were taken (Fig. 2a). The morphology of biochar obtained as a result of high-temperature treatment exhibited a porous, fibrous structure, consistent with observations presented in other sources (Vaghela et al., 2023). The size and shape of the obtained BC particles varied, with sizes ranging from approx. several microns to approx. several hundred microns. This diversity was caused by the use of mechanical modification with a biomass ball mill, contributing to non-uniform straw fragmentation.

The ground biomass contained both larger fragments of straw fibers and smaller particles resulting from the breakdown of cell walls. After pyrolysis, the fibrous fragments had a porous layered structure, while smaller particles showed a heterogeneous shape with jagged and sharp edges. The presence of honeycomb pores in the biochar structure can cause mechanical bonding of the polymer with the BC and the penetration of rubber between the pores of the filler, making it a very effective reinforcing agent (Ikram et al., 2016). There were no notable differences observed in the morphology of biochar obtained at 600 and 900 °C.

For comparison, SEM images of commercially used N550 carbon black were also taken. It was characterized by spherical primary particles with nanometer sizes. However, as observed in images at lower magnification, CB particles tended to form structures with sizes of several dozen microns.

Based on images of fractures of filled vulcanizates (Fig. 3b), the degree of dispersion of carbon additives in NR was assessed. The sample containing CB was characterized by a uniform distribution of carbon black particles in the material structure. The sizes of carbon black aggregates and agglomerates present in SEM images did not exceed several microns. In contrast, in vulcanizates containing biochar, structures with sizes below 1 μm appeared, as well as larger aggregates of filler or primary particles with sizes of several μm. This was mainly due to the diverse morphology of carbon biofillers. It should be emphasized that the images showed a good connection of biochar with NR, with no delaminations or discontinuities of the rubber at the filler-polymer interface observed. This characteristic is highly advantageous in terms of strength properties.

3.5. *Rheometric properties of the NR mixture*

In order to determine the process characteristics and initial differences in the properties provided by carbon black and biochar fillers, rheometric measurements were carried out. The obtained results are summarized in Table 4. The rheometric curves of NR composites are included in supplementary materials (Fig S2.).

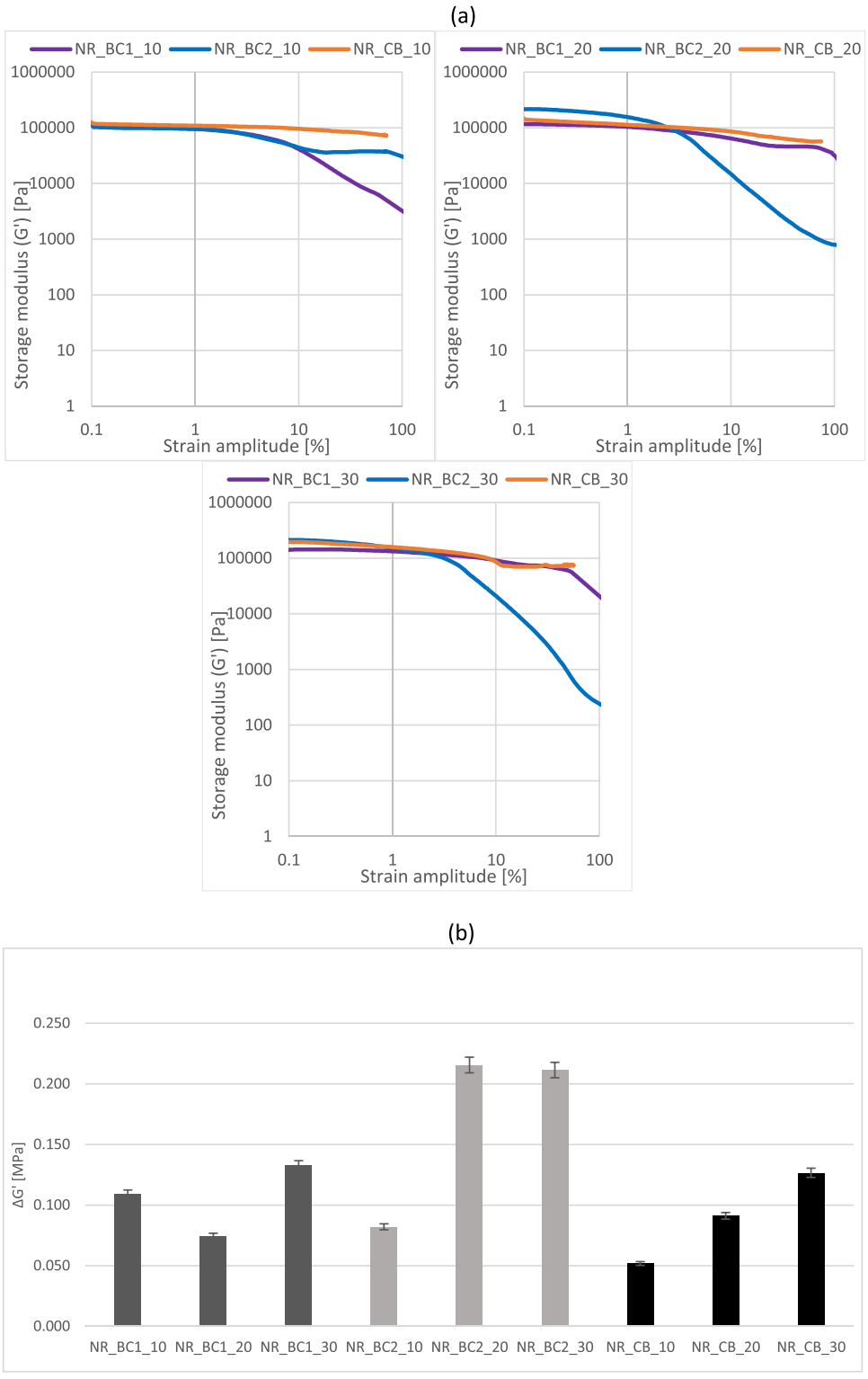

Fig. 3. Plot of storage modulus versus strain (a). Values of the Payne effect for composites NR (b).

Minimum torque (M_{min}) is a parameter related to the viscosity of the composition. As viscosity, i.e. the physical interactions between the mixture components, increases, a greater torque must be applied to achieve the same deformation. In processing, this means greater energy expenditure for manipulating the unvulcanized mixture. Compared to the NR0 mixture without any filler, the addition of filler reduced this value. However, the amount had no significant effect and no clear correlation can be established between the filler content and the increase or decrease in torque.

Increased M_{max} indicates an increase in the total network structure, influenced by filler-filler interactions, polymer-filler interactions, and covalent cross-links between rubber macromolecules created during vulcanization (Raju et al., 2021). The highest values of maximum torque recorded during vulcanization were observed for mixtures containing carbon filler obtained during straw pyrolysis, regardless of the heat treatment temperature. This means that these biocomposites were

Table 4
Rheometric characteristics of NR composites with 10 phr (a), 20 phr (b) and 30 phr (c) amount of carbon fillers.

(a)					
Sample	M_{min} [dNm]	M_{max} [dNm]	ΔM [dNm]	t_5 [min]	t_{90}[min]
NR0	0,58	2,87	2,29	0,96	4,63
NR_CB_10	0,39	3,00	2,61	0,79	4,04
NR_BC1_10	0,38	4,78	4,40	0,42	2,02
NR_BC2_10	0,49	4,94	4,45	0,46	2,21
(b)					
Sample	M_{min} [dNm]	M_{max} [dNm]	ΔM [dNm]	t_5 [min]	t_{90}[min]
NR0	0,58	2,87	2,29	0,96	4,63
NR_CB_20	0,28	3,27	2,99	0,75	4,36
NR_BC1_20	0,34	6,05	5,71	0,45	2,24
NR_BC2_20	0,36	6,10	5,74	0,50	2,49
(c)					
Sample	M_{min} [dNm]	M_{max} [dNm]	ΔM [dNm]	t_5 [min]	t_{90}[min]
NR0	0,58	2,87	2,29	0,96	4,63
NR_CB_30	0,48	4,18	3,70	0,70	4,24
NR_BC1_30	0,36	6,92	6,56	0,47	2,40
NR_BC2_30	0,25	6,51	6,26	0,52	2,94

characterized by the most extensive system of spatial connections, which should be reflected in their strength properties.

The torque gain refers to the variance between the maximum and minimum torque recorded during the test (ΔM). This value indicates the degree of vulcanization of the sample and can indirectly asses the cross-linking density of the rubber. In the process of vulcanization, cross-links are formed between rubber macromolecules and interactions between the polymer and the filler are created. All samples containing filler showed higher growth values than the unfilled elastomer mixture. Analyzing the above data, it can be concluded that the commercial carbon filler showed the lowest growth values compared to all other tested additives. As the filler content increased, a rise in torque was evident across all samples. Moreover, there was no noteworthy disparity in the impact on the cross-linking process between the effects of biochar obtained at varying pyrolysis temperatures; the increment values were similar. Carbon fillers made from plant biomass contained basic calcium, potassium and magnesium compounds (Fig S3.), which could increase the effectiveness of the cross-linking reaction (Hayeemasae et al., 2022). Alkaline compounds such as calcium and magnesium oxides are a potential alternative to zinc oxide used as an activator in the process of sulfur rubber vulcanization. Their activity in the vulcanization process has been confirmed in several scientific publications, which have demonstrated both their effectiveness as an activator and their ability to create structures and their accelerating effect on the reaction of rubber with sulfur (Feldstein et al., 1958; Heideman et al., 2005). These compounds can act catalytically, reducing the time required for vulcanization and the optimal vulcanization time (t_{90}), which has been confirmed for mixtures containing biochar. Generally, the use of a filler shortened the vulcanization time, and the use of biochar fillers further reduced this parameter. This effect could be due to the presence of active functional groups in carbon fillers, capable of catalyzing vulcanization. During the production process and their storage, the surface of carbon fillers is oxidized, which results in the formation of functional groups containing oxygen, such as carboxyl, hydroxyl or phenolic. The presence of such groups on the surface of biochar was confirmed by Bardha's team in FTIR studies (Bardha et al., 2024). In addition, free radicals may be present on the surface of carbon additives (Y. Zhang et al., 2020). These chemical properties make the surface of these filler particles chemically active. The smallest amount of biochar had the greatest impact on shortening the vulcanization time. Increasing the load with this filler contributes to the extension of the t_{90} parameter. The active compounds and functional groups in the BC probably increased the effectiveness of the vulcanization reaction. On the other hand, carbon filler particles, due to their extensive specific surface area, could absorb components of the cross-linking agent, resulting in their less efficient utilization in the cross-linking process and, consequently, a slower vulcanization rate. Poorer dispersion of the rubber mixture components with a higher additive load was also significant.

3.6. Differential scanning calorimetry

To more precisely determine the influence of the utilized carbon fillers on the cross-linking characteristics of NR composition, measurements were carried out using differential scanning calorimetry (DSC). The impact of different types of biochar on the vulcanization temperature and the enthalpy of this process was examined, and the obtained parameters were compared with the traditional composition using carbon black. Additionally, the influence of the biofillers and carbon black on the glass transition temperature (Tg) of the natural rubber mixtures was specified. The results of the DSC analysis are illustrated in Table 5. The DSC curves of NR vulcanizates are included in the supplementary materials (Fig S4.)

For all samples, two main thermal processes were observed in the DSC curve. The first, occurring at negative temperatures, corresponded to the glass transition, i.e., a second-order phase transition. The Tg value of the reference mixture was −61.5 °C; the addition of the filler, both in the form of carbon black and biochar, caused a shift in Tg toward lower temperatures. Due to the high surface activity and "extended structure" of biochar, the NR polymer chains were easily adsorbed onto the surface of the BC particles and trapped inside their agglomerates. Therefore, the mobility of rubber molecules was significantly limited by the strong bonding at the filler-rubber interface. As a result, the Tg of rubber composites containing carbon fillers changed from −61.5 °C to as low as −65.5 °C. Such a change in Tg sufficiently demonstrated the significant interfacial interactions between BC and polymer. Furthermore, the porous structure of the resulting biochar could cause the rubber to penetrate between the free spaces of the filler, leading to the stiffening of NR macromolecules, and ultimately a decrease in the Tg temperature of the biocomposites. The activity of biochar obtained from waste lignin in interactions with the SBR elastomer was confirmed by other authors (Jiang et al., 2020), who also observed a shift in the Tg temperature of the materials from 38.5 °C to –32.5 °C. Analyzing the further course of the DSC curve (Fig. 1), a change in the heat flux was observed, which was associated with the cross-linking of the NR mixtures. For the tested compositions, it was a one-stage exothermic process, occurring within a temperature range that depended on the formulation of NR mixtures, mainly on the type of carbon additive used.

Cross-linking of the reference rubber mixture occurred at temperatures from 171 °C to 215 °C with an enthalpy (ΔH) of approximately 14.13 J/g. The introduction of a commercial filler did not notably influence the cross-linking temperature range of NR compounds, while the cross-linking enthalpy (ΔH) was reduced compared to the unfilled system. However, the addition of biochar, regardless of the type, significantly influenced the vulcanization temperature. The cross-linking initiation temperature was reduced by approximately 15–16 °C

Table 5
DSC analysis of rubber mixes with 30 phr of fillers.

Sample	Content of filler [phr]	T_{onset} [°C]	T_{endset} [°C]	ΔH [J/g]	Tg [°C]
NR0	0	171,6	215,2	14,13	−61,5
NR_CB_30	30	172,4	209,9	6,75	−64,4
NR_BC1_30	30	155,0	214,7	15,80	−65,5
NR_BC2_30	30	154,1	223,7	17,47	−64,0

T_{onset} - Initial temperature of vulcanization.
T_{endset} - Final vulcanization temperature.
ΔH - Enthalpy of the vulcanization process.
Tg - Glass transition temperature.

compared to the previously discussed NR blends. Moreover, both BC1 and BC2 increased the energetic effect of the vulcanization process compared to the reference compositions. This confirmed the beneficial effect of using biochar as an alternative elastomer filler on the cross-linking reaction. Mineral substances contained in fillers obtained from biomass could have had a significant impact on the vulcanization process of biocomposites. Literature suggests that basic metal oxides present in the residues after heat treatment of biomass can have a catalytic effect on the sulphur vulcanization process, resulting in a better connection of rubber macromolecules and the filler (da Costa et al., 2003).

3.7. Cross-linking density

The cross-linking density (ν_e) is a crucial parameter for the properties of rubber vulcanizates, due to the correlation between the cross-linked structure and the final characteristic of the finished material. Often, a higher cross-linking density results in an enhancement of the mechanical strength of the rubber, but at the same time, such a material may be less flexible. Table 6 presents the results calculated for the ν_e value of the produced biocomposites.

The cross-linking density depends mainly, but not solely, on the cross-linking unit used. The introduced filler may influence the cross-linking process as long as it contains active ingredients that react during the formation of the spatial network.

The results indicate that the commercial carbon additive had a very small impact on the ν_e of the biocomposites. The increase in this parameter's value for these materials was probably related to the occurrence of additional filler-polymer interactions. Functional groups on the CB surface can interact with the elastomer, thereby increasing the concentration of effective network nodes.

Comparing biochar obtained from plant sources in the pyrolysis process to commercial carbon black and an unfilled elastomer mixture, an increase in the ν_e value can be indicated. This confirms the previous conclusions from the rheometric study and comparison of the torque increase. Carbon material for high-technology applications originating from biological sources, apart from elemental carbon itself, may also contain several other substances from both the plants themselves and the reactions occurring during its preparation process. These substances can be both an obstacle and an advantage depending on the material's intended use. As previously noted, compounds derived from plant biofillers catalytically influence the sulfur vulcanization process, which in turn may also influence the cross-linking density. Moreover, interactions at the interface between the additive particles and the rubber may play an important role, potentially benefiting the mechanical properties of these materials. Tensile strength is strictly dependent on the additive-polymer interfaces, as well as on the distribution and transfer of stresses between the components of the composition. Moreover, according to the theory proposed by Bueche (Buche and Silberstein, 2021), strong filler-polymer bonds constitute an extension of the spatial structure of the composite and can be considered physical connections completing the network.

Table 6
The value of cross-linking density of composites along with statistical analysis.

Sample	Content of filler [phr]	$\nu_e \cdot 10^{-5}$ mol/cm^3	Standard deviation	Variance	p-value
NR0	0	1,35	0,09	-	-
NR_CB	10	1,27	0,03	$1{,}37 \cdot 10^{-13}$	$6{,}46 \cdot 10^{-9}$
NR_BC1		2,50	0,03	$1{,}53 \cdot 10^{-13}$	
NR_BC2		2,51	0,12	$1{,}80 \cdot 10^{-12}$	
NR_CB	20	1,37	0,02	$7{,}10 \cdot 10^{-14}$	$1{,}84 \cdot 10^{-9}$
NR_BC1		3,35	0,16	$3{,}60 \cdot 10^{-12}$	
NR_BC2		3,33	0,05	$3{,}04 \cdot 10^{-13}$	
NR_CB	30	1,74	0,06	$5{,}05 \cdot 10^{-13}$	$5{,}66 \cdot 10^{-11}$
NR_BC1		4,12	0,10	$1{,}26 \cdot 10^{-12}$	
NR_BC2		3,33	0,05	$3{,}04 \cdot 10^{-13}$	

3.8. Mechanical properties in static conditions

One of the most important studies directly related to the functionality of newly designed materials is the determination of their mechanical properties. In the case of elastomeric composite materials, these focus primarily on stress values at 300 % deformation, mechanical strength at break and elongation at break, as shown in Table 7.

The obtained results suggest that with the increase in the content of carbon fillers, the SE_{300} value increased for all tested vulcanizate samples, regardless of the type of additive used. However, considering biochar additives (BC1 and BC2), the obtained SE_{300} values were similar for individual filler contents (Table 5). In contrast, the commercial filler showed lower stress values compared to biochar, indicating the strengthening effect of biofillers in the range of low deformations and its active nature. Understandably, all filled composites had higher stress than the unfilled reference sample (NR0).

According to the data in Table 7, an increase in the degree of rubber filling resulted in the strengthening of all tested vulcanizates compared to the unfilled system. There is a correlation between the ν_e value described in the previous section and the TS values. Samples with the highest cross-linking density, i.e. vulcanizates with applied BC, also showed the highest TS value. This phenomena could have been influenced by the hydrodynamic effect, filler-filler, or additive-elastomer connections. Composites with the least extensive spatial network, i.e. filled with commercial carbon black, were characterized by the lowest mechanical strength.

Table 7
Mechanichal properties of elastomer composites filled with carbon additives.

Sample	Content of filler [phr]	SE_{300} [MPa]	Standard deviation	Variance	p-value
NR0	0	1,00	0,02	-	-
NR_CB	10	1,33	0,03	0,0009	$3{,}09 \cdot 10^{-9}$
NR_BC1		2,08	0,07	0,0052	
NR_BC2		2,10	0,03	0,0006	
NR_CB	20	3,21	0,08	0,0068	0,03
NR_BC1		3,26	0,07	0,0044	
NR_BC2		3,35	0,02	0,0005	
NR_CB	30	3,41	0,10	0,0109	$9{,}25 \cdot 10^{-8}$
NR_BC1		4,35	0,09	0,0089	
NR_BC2		4,47	0,07	0,0056	
Sample	**Content of filler [phr]**	**TS [MPa]**	**Standard deviation**	**Variance**	**p-value**
NR0	0	6,71	0,30	-	-
NR_CB	10	12,60	0,64	0,41	$3{,}69 \cdot 10^{-7}$
NR_BC1		19,40	0,59	0,35	
NR_BC2		19,90	0,98	0,95	
NR_CB	20	14,63	0,30	0,09	$3{,}08 \cdot 10^{-9}$
NR_BC1		21,08	0,43	0,18	
NR_BC2		21,30	0,48	0,23	
NR_CB	30	13,48	0,74	0,55	$7{,}73 \cdot 10^{-7}$
NR_BC1		19,48	0,59	0,35	
NR_BC2		18,38	0,59	0,35	
Sample	**Content of filler [phr]**	**EB [%]**	**Standard deviation**	**Variance**	**p-value**
NR0	0	729	23	-	-
NR_CB	10	738	15	223	0,0429
NR_BC1		755	9	87	
NR_BC2		765	16	270	
NR_CB	20	650	10	103	0,0004
NR_BC1		698	12	134	
NR_BC2		679	9	84	
NR_CB	30	567	30	878	0,0013
NR_BC1		638	8	70	
NR_BC2		618	11	118	

Moreover, it is evident that the optimal filling value is 20phr of the additive, regardless of its type. The obtained tensile strength values are the highest for these filler amounts. The mechanical strength values for the samples of vulcanizates filled with biochar from plant sources were much higher for those with commercially used carbon black filler, reaching exactly 21.3 MPa for the best NR_BC2_20 sample. This is an increase of 46 % compared to the NR_CB_20 sample and 21.7 % compared to the unfilled vulcanizate (Table 7).

The relative EB value of the filled elastomer biocomposites was consistent with the theory: with the increase in additive content within the elastomeric medium, the elongation of the vulcanizates decreases (Table 7). Therefore, the highest recorded EB values were characteristic of vulcanizates with the lowest degree of filling.

3.9. Thermogravimetric analysis

Thermogravimetric analysis of vulcanizates allowed to determine their thermal stability and detailed the exact course of thermal decomposition of the composites. Characteristic parameters for the reference sample (NR0) and vulcanizates containing 30 phr of additives are presented in Table 8. The TG and DTG curves of NR composites are included in the supplementary materials (Fig S5.)

The decomposition process of natural rubber vulcanizates occurred in one stage, the temperature at the beginning of decomposition of the reference sample, defined as 5 % mass loss, was 329 °C, the addition of commercial carbon black slightly increased the thermal stability of the elastomer by several degrees Celsius. However, the addition of carbon filler obtained from straw did not affect the initial decomposition temperature of the sample (T_5). The same relationship was noted for the T_{50} parameter. The addition of biochar to natural rubber caused a slight shift in the temperature corresponding to the maximum intensity of material decomposition ($T_{peakDTG}$) towards lower values. The weight loss during the initial stage of thermogravimetric analysis (25–600 °C) was mainly associated with the thermal decomposition of the elastomer. For the reference sample, a mass loss of 93 % was obtained, while vulcanizates containing carbon fillers showed a mass loss of 73–75 %, corresponding to the elastomeric matrix content in the compositions. After changing the atmosphere (from argon to air) and carrying out measurements at a temperature above 600 °C, the carbon in the composite samples burned, reflected in the mass loss of the samples. A slightly higher mass conversion value of 21 %, was recorded for the sample filled with CB compared to vulcanizates reinforced with biochar, which had a $\Delta m_{600-900}$ value of 16 %. This was due to the present of additional thermally stable phyto-ashes in the biochar, constituting the residue after analysis. This was confirmed by the R_{900} parameter results, which clearly showed differences in the amount of residues after the decomposition of vulcanizates. Composites containing carbon fillers of natural origin had an 8–9 % ash content remaining after sample decomposition. Previous research showed that phyto-ash produced from straw is rich in calcium, magnesium, and silicon compounds (Masłowski et al., 2021). The solid residue after the decomposition of the remaining samples amounted to approximately 5 %, likely consisting of ZnO used as an activator and ash remaining after burning natural rubber.

Table 8
Thermogravimetric analysis of the composites.

Sample	T_5 °C	T_{50} °C	$T_{peakDTG}$ °C	Δm_{25-600} %	$\Delta m_{600-900}$ %	R_{900} %
NR0	329	390	388	93,4	0,8	5,9
NR_CB_30	342	401	388	72,9	21,7	5,4
NR_BC1_30	332	393	382	75,4	16,7	7,9
NR_BC2_30	329	393	382	74,8	16,2	9,0

3.10. Dynamic mechanical analysis

Using a rotational rheometer, the effects occurring during dynamic, i.e. time-varying, deformation of the rubber were measured. The result of the study was the correlation between the storage modulus G′ and the percentage of deformation, as is illustrated in Fig. 3a.

Dynamic tests were conducted at a constant temperature and strain frequency, with a variable strain amplitude. The elastic component of the dynamic modulus G′ decreased after exceeding a certain strain amplitude, known as the Payne Effect. The Payne Effect may be related to factors such as agglomeration/deagglomeration of filler aggregates, disintegration/reformation of the additive "network", polymer-filler interactions, desorption of macromolecules chains occluded by the filler, and disentangling of adsorbed chains.

The attached figures clearly show that all vulcanizates samples containing carbon black, regardless of their amount, had significantly different G′ curve compared to samples filled with biochar. Carbon black, as a reinforcing filler, had a high ability to create polymer-filler interactions, which are stronger than filler-filler interactions and occur less frequently with CB. This type of network made the composites stiff and at larger deformations above 100 %, the material slipped out of the measuring device. A smaller share of filler-filler interactions resulted in an insignificant decrease in the G′ value, reflected in a small ΔG value (Fig. 3b). Higher modulus values with increasing loading can be attributed to a poorer degree of dispersion of the additives in the rubber.

Conversely, for biocomposites, a significant decrease in the storage modulus with increasing deformation was noted. This result might be due to well-developed "secondary biofiller structure" in vulcanizates. The existing filler-filler interactions were destroyed after exceeding a certain deformation limit, reducing the G′ value. The highest ΔG values were obtained for samples NR_BC1_20 and NR_BC2_30. There is no correlation between the biochar content and the Payne effect achieved, unlike with vulcanizates with carbon black. The variety and diversified morphology of these biofillers could contribute to the creation of more complex structural forms, thus influencing the dispersion properties of the vulcanizates, and the obtained results of the Payne effect.

3.11. Thermo-oxidative (TO) aging characteristics of vulcanizates

The study of the aging resistance of the produced elastomeric biocomposites to simulated TO aging processes was determined based on a comparative analysis of how the aging factor affects the changes in cross-linking density and mechanical parameters of the composites tested both before and after aging. Table 9 presents the results of changes in the ν_e value of vulcanizates after thermo-oxidative degradation processes.

The results indicates that vulcanizates containing bio-based additives were less resistant to the effects of aging. The $\Delta\nu e$ values reached up to 50 % in more heavily filled composites, in contrast to the samples filled with carbon black, where the change in cross-linking density did not exceed 15 %. Nevertheless, considering the initial higher ν_e values of biocomposites with biochar, the difference between vulcanizates containing a commercial filler and those with innovative biobased filler was not dramatic. Moreover, all filled samples still had higher values than the unfilled NR0 sample, indicating better resistance of these composites compared to the reference material.

One of the most important features of rubber products are their mechanical properties, which guarantee long-term, trouble-free use. Table 9 presents the results of mechanical tests after exposure to the aging factor, i.e. increased temperature and oxygen.

The impact of TO aging on the mechanical strength of rubber biocomposites is reliably illustrated by the aging factor (K), which determines the change in stress-strain behavior of the sample. It depends on the values of TS and EB of vulcanizates subjected to a specific aging process. The numerical results are depicted in Table 9. The K value represents the ratio of the EB and TS values measured after and before

Table 9
The influence of thermo-oxidative aging processes on tested properties of NR vulcanizates.

Sample	Content of filler [phr]	Cross-linking density			Mechanical properties			
		Before aging $\nu_e \cdot 10^{-5}$ [mol/cm^3]	After aging	$\Delta\nu_e$ [%]	SE_{300} [MPa]	TS [MPa]	EB [%]	K [-]
NR0	0	1,35	1,28	−5 %	1,1	7,27	550	0,82
NR_CB	10	1,27	1,47	15 %	2	9	533	0,52
	20	1,37	1,5	9 %	2,8	9,22	525	0,51
	30	1,74	1,93	11 %	5,1	8,9	468	0,54
NR_BC1	10	2,5	1,79	−28 %	2,1	7,2	613	0,3
	20	3,35	1,89	−44 %	2,6	6,5	550	0,24
	30	4,12	2,2	−46 %	3	5,92	520	0,25
NR_BC2	10	2,51	1,64	−35 %	1,9	8,34	594	0,33
	20	3,33	1,81	−46 %	2,5	6,9	540	0,26
	30	3,83	1,59	−59 %	2,5	5,98	499	0,26

aging. The closer it is to unity, the more resistant the material is to degradation, indicating that the mechanical properties have not changed significantly.

Samples filled with commercial carbon black were the most resistant to thermo-oxidative aging, with K values ranging from 0.50 to 0.54. Increasing the filler share to 30 phr had a positive effect on the anti-aging protection of composites. Biofillers exhibited significantly lower K parameter values (from 0.24 to 0.33). Biochar obtained from pyrolysis at 900 °C had slightly better properties in this respect. Vulcanizates filled with materials obtained from natural sources were characterized by low resistance to aging, likely due to the presence of non-carbon components. Metal ions with variable valency may have particularly influence the rate of rubber aging (Zhao et al., 2023).

For the unfilled vulcanizate, the K parameter reached 0.82, indicating that the material could be cross-linked at elevated temperatures, which increased its mechanical properties.

As aging tests have shown, the resistance of biocomposites to thermo-oxidative conditions is surprisingly low. The issue of protecting composites against external degradation factors requires further work. Potential directions for this work include the use of compounds with the ability to chelate metals. Such a procedure could reduce the activity of compounds contained in biochar that accelerate the aging of the material. Additionally, biochar modifications can be used to control the qualitative composition of the filler.

4. Conclusion

Pyrolysis of straw at 600 °C was found to be as effective as at higher temperatures, with similar mass loss in the resulting biochar samples B1 and B2. Elemental analysis showed that higher pyrolysis temperatures increased carbon content due to the intensified release of volatile substances at 900 °C. The smallest fraction (<0.045 mm) dominated the granulometric analysis, suggesting better dispersion in elastomer matrices and potential strengthening effects, making biochar a viable alternative to commercial carbon black.

While both biochar and carbon black share high carbon content, their effects on cross-linking and mechanical properties differ. Biochar composites showed better mechanical strength but higher aging susceptibility. An optimal biochar content of 20 phr in vulcanizates enhanced tensile strength, though aging resistance was lower, indicating the need for anti-aging strategies to improve biochar's viability as a carbon black substitute.

Biochar offers additional benefits, being renewable and potentially carbon-neutral, especially when produced using renewable energy. However, its environmental impact depends on post-use combustion. Further research is needed to optimize biochar's production, extraction, and application in composites.

The composition, origin, and amount of bio-additives like biochar significantly influence composite properties. While large quantities of bio-waste provide opportunities for reuse, more research is required to fully understand how these factors affect the processing and functionality of polymer biocomposites.

CRediT authorship contribution statement

Krzysztof Strzelec: Supervision. **Justyna Miedzianowska-Masłowska:** Writing – review & editing, Writing – original draft, Visualization, Validation, Resources, Methodology, Investigation, Formal analysis, Data curation, Conceptualization. **Marcin Masłowski:** Writing – review & editing, Writing – original draft, Resources, Methodology, Investigation, Conceptualization. **Maciej Delekta:** Writing – original draft, Investigation.

Declaration of Competing Interest

The authors declare that they have no known competing financial interests or personal relationships that could have appeared to influence the work reported in this paper.

Data availability

Data will be made available on request.

Appendix A. Supporting information

Supplementary data associated with this article can be found in the online version at doi:10.1016/j.indcrop.2024.119629.

References

Abd El-Aziz, M.E., Shafik, E.S., Tawfic, M.L., Morsi, S.M.M., 2022. Biochar from waste agriculture as reinforcement filer for styrene/butadiene rubber. Polym. Compos. 43, 1295–1304. https://doi.org/10.1002/pc.26448.

Aboughaly, M., Babaei-Ghazvini, A., Dhar, P., Patel, R., Acharya, B., 2023. Enhancing the potential of polymer composites using biochar as a filler: a review. Polymers (Basel) 15, 3981. https://doi.org/10.3390/polym15193981.

Al-Rumaihi, A., Shahbaz, M., Mckay, G., Mackey, H., Al-Ansari, T., 2022. A review of pyrolysis technologies and feedstock: a blending approach for plastic and biomass towards optimum biochar yield. Renew. Sustain. Energy Rev. 167, 112715 https://doi.org/10.1016/j.rser.2022.112715.

Anerao, P., Kulkarni, A., Munde, Y., Shinde, A., Das, O., 2023. Biochar reinforced PLA composite for fused deposition modelling (FDM): a parametric study on mechanical performance. Compos. Part C: Open Access 12, 100406. https://doi.org/10.1016/j.jcomc.2023.100406.

Ayadi, R., Koubaa, A., Braghiroli, F., Migneault, S., Wang, H., Bradai, C., 2020. Effect of the pyro-gasification temperature of wood on the physical and mechanical properties of biochar-polymer biocomposites. Materials 13, 1327. https://doi.org/10.3390/ma13061327.

Bardha, A., Kurian, J.K., Gariépy, Y., Prasher, S., Cornejo, R.L.B., Khirpin, C., Mehlem, J., Dumont, M.-J., 2024. Physicochemical characterization of different steam activations of corn stover biochar and their reinforcement of styrene-butadiene rubber composites. Waste Biomass Valoriz. 15, 2285–2298. https://doi.org/10.1007/s12649-023-02287-1.

Bartoli, M., Arrigo, R., Malucelli, G., Tagliaferro, A., Duraccio, D., 2022. Recent advances in biochar polymer composites. Polymers 14, 2506. https://doi.org/10.3390/polym14122506.

Björnsson, L., Prade, T., 2021. Sustainable cereal straw management: use as feedstock for emerging biobased industries or cropland soil incorporation? Waste Biomass Valoriz. 12, 5649–5663. https://doi.org/10.1007/s12649-021-01419-9.
Bridgwater, A.V., 2012. Review of fast pyrolysis of biomass and product upgrading. Biomass Bioenergy 38, 68–94. https://doi.org/10.1016/j.biombioe.2011.01.048.
Buche, M.R., Silberstein, M.N., 2021. Chain breaking in the statistical mechanical constitutive theory of polymer networks. J. Mech. Phys. Solids 156, 104593. https://doi.org/10.1016/j.jmps.2021.104593.
Burhenne, L., Messmer, J., Aicher, T., Laborie, M.-P., 2013. The effect of the biomass components lignin, cellulose and hemicellulose on TGA and fixed bed pyrolysis. J. Anal. Appl. Pyrolysis 101, 177–184. https://doi.org/10.1016/j.jaap.2013.01.012.
Chen, Y.-H., Schmid, M., Chang, C.-C., Chang, C.-Y., Scheffknecht, G., 2020. Lab-scale investigation of palm shell char as tar reforming catalyst. Catalysts 10, 476. https://doi.org/10.3390/catal10050476.
da Costa, H.M., Visconte, L.L.Y., Nunes, R.C.R., Furtado, C.R.G., 2003. Rice husk ash filled natural rubber. III. Role of metal oxides in kinetics of sulfur vulcanization. J. Appl. Polym. Sci. 90, 1519–1531. https://doi.org/10.1002/app.12684.
Fan, Y., Fowler, G.D., Zhao, M., 2020. The past, present and future of carbon black as a rubber reinforcing filler – a review. J. Clean. Prod. 247, 119115 https://doi.org/10.1016/j.jclepro.2019.119115.
Feldstein, M., Orlovsky, P., Dogadkin, B., 1958. The role of metal oxides as activators of vulcanization. Rubber Chem. Technol. 31, 526–538. https://doi.org/10.5254/1.3542304.
Gabhane, J.W., Bhange, V.P., Patil, P.D., Bankar, S.T., Kumar, S., 2020. Recent trends in biochar production methods and its application as a soil health conditioner: a review. SN Appl. Sci. 2, 1307. https://doi.org/10.1007/s42452-020-3121-5.
Garg, S., Das, P., 2020. Microporous carbon from cashew nutshell pyrolytic biochar and its potential application as CO2 adsorbent. Biomass Convers. Biorefin 10, 1043–1061. https://doi.org/10.1007/s13399-019-00506-1.
Greenough, S., Dumont, M.J., Prasher, S., 2021. The physicochemical properties of biochar and its applicability as a filler in rubber composites: a review. Mater. Today Commun. https://doi.org/10.1016/j.mtcomm.2021.102912.
Grønli, M.G., Várhegyi, G., Di Blasi, C., 2002. Thermogravimetric analysis and devolatilization kinetics of wood. Ind. Eng. Chem. Res 41, 4201–4208. https://doi.org/10.1021/ie0201157.
Guo, X., Liu, H., Zhang, J., 2020. The role of biochar in organic waste composting and soil improvement: a review. Waste Manag. 102, 884–899. https://doi.org/10.1016/j.wasman.2019.12.003.
Gupta, A., Mohanty, A.K., Misra, M., 2022. Biocarbon from spent coffee ground and their sustainable biocomposites with recycled water bottle and bale wrap: a new life for waste plastics and waste food residues for industrial uses. Compos. Part A Appl. Sci. Manuf. 154, 106759 https://doi.org/10.1016/j.compositesa.2021.106759.
Haleem, N., Khattak, A., Jamal, Y., Sajid, M., Shahzad, Z., Raza, H., 2022. Development of poly vinyl alcohol (PVA) based biochar nanofibers for carbon dioxide (CO2) adsorption. Renew. Sustain. Energy Rev. 157, 112019 https://doi.org/10.1016/j.rser.2021.112019.
Hayeemasae, N., Masa, A., Othman, N., Surya, I., 2022. Viable properties of natural rubber/halloysite nanotubes composites affected by various silanes. Polymers 15, 29. https://doi.org/10.3390/polym15010029.
Heideman, G., Noordermeer, J.W.M., Datta, R.N., Van Baarle, B., 2005. Effect of metal oxides as activator for sulphur vulcanisation in various rubbers. KGK Kautsch. Gummi Kunstst. 58.
Ikeda, Y., 2014. Understanding network control by vulcanization for sulfur cross-linked natural rubber (NR). In: Chemistry, Manufacture and Applications of Natural Rubber. Elsevier, pp. 119–134. https://doi.org/10.1533/9780857096913.1.119.
Ikram, S., Das, O., Bhattacharyya, D., 2016. A parametric study of mechanical and flammability properties of biochar reinforced polypropylene composites. Compos Part A Appl. Sci. Manuf. 91, 177–188. https://doi.org/10.1016/j.compositesa.2016.10.010.
Jiang, C., Bo, J., Xiao, X., Zhang, S., Wang, Z., Yan, G., Wu, Y., Wong, C., He, H., 2020. Converting waste lignin into nano-biochar as a renewable substitute of carbon black for reinforcing styrene-butadiene rubber. Waste Manag. 102, 732–742. https://doi.org/10.1016/j.wasman.2019.11.019.
Kalak, T., 2023. Potential use of industrial biomass waste as a sustainable energy source in the future. Energies 16, 1783. https://doi.org/10.3390/en16041783.
Kim, K.H., Kim, J.-Y., Cho, T.-S., Choi, J.W., 2012. Influence of pyrolysis temperature on physicochemical properties of biochar obtained from the fast pyrolysis of pitch pine (Pinus rigida). Bioresour. Technol. 118, 158–162. https://doi.org/10.1016/j.biortech.2012.04.094.
Kumar, R., Singh, S., Singh, O.V., 2008. Bioconversion of lignocellulosic biomass: biochemical and molecular perspectives. J. Ind. Microbiol Biotechnol. 35, 377–391. https://doi.org/10.1007/s10295-008-0327-8.
Maciejewska, M., Sowińska-Baranowska, A., 2022. Bromide and chloride ionic liquids applied to enhance the vulcanization and performance of natural rubber biocomposites filled with nanosized silica. Nanomaterials 12, 1209. https://doi.org/10.3390/nano12071209.
Masłowski, M., Miedzianowska, J., Strzelec, K., 2017. Natural rubber biocomposites containing corn, barley and wheat straw. Polym. Test. 63, 84–91. https://doi.org/10.1016/j.polymertesting.2017.08.003.
Masłowski, M., Miedzianowska, J., Delekta, M., Czylkowska, A., Strzelec, K., 2021. Natural rubber biocomposites filled with phyto-ashes rich in biogenic silica obtained from wheat straw and field horsetail. Polym. (Basel) 13. https://doi.org/10.3390/polym13071177.
Mohd Hasan, M., Bachmann, R., Loh, S., Manroshan, S., Ong, S., 2019. Effect of pyrolysis temperature and time on properties of palm kernel shell-based biochar. IOP Conf. Ser. Mater. Sci. Eng. 548, 012020 https://doi.org/10.1088/1757-899X/548/1/012020.
Nagarajan, V., Mohanty, A.K., Misra, M., 2016. Biocomposites with size-fractionated biocarbon: influence of the microstructure on macroscopic properties. ACS Omega 1, 636–647. https://doi.org/10.1021/acsomega.6b00175.
Peterson, S.C., Chandrasekaran, S.R., Sharma, B.K., 2016. Birchwood biochar as partial carbon black replacement in styrene–butadiene rubber composites. J. Elastomers Plast. 48, 305–316. https://doi.org/10.1177/0095244315576241.
Peterson, S.C., Kim, S., 2020. Reducing biochar particle size with nanosilica and its effect on rubber composite reinforcement. J. Polym. Environ. 28, 317–322. https://doi.org/10.1007/s10924-019-01604-x.
Quosai, P., Anstey, A., Mohanty, A.K., Misra, M., 2018. Characterization of biocarbon generated by high- and low-temperature pyrolysis of soy hulls and coffee chaff: for polymer composite applications. R. Soc. Open Sci. 5, 171970 https://doi.org/10.1098/rsos.171970.
Raju, G., Khalid, M., Shaban, M.M., Azahari, B., 2021. Preparation and characterization of eco-friendly spent coffee/ENR50 biocomposite in comparison to carbon black. Polymers 13, 2796. https://doi.org/10.3390/polym13162796.
Ramaswamy, R., Gurupranes, S.V., Kaliappan, S., Natrayan, L., Patil, P.P., 2022. Characterization of prickly pear short fiber and red onion peel biocarbon nanosheets toughened epoxy composites. Polym. Compos 43, 4899–4908. https://doi.org/10.1002/pc.26735.
Ronsse, F., van Hecke, S., Dickinson, D., Prins, W., 2013. Production and characterization of slow pyrolysis biochar: influence of feedstock type and pyrolysis conditions. GCB Bioenergy 5, 104–115. https://doi.org/10.1111/gcbb.12018.
Sarkar, J.K., Wang, Q., 2020. Different pyrolysis process conditions of south asian waste coconut shell and characterization of gas, bio-char, and bio-oil. Energies 13, 1970. https://doi.org/10.3390/en13081970.
Scapin, E., Maciel, G.P., da, S., Polidoro, A.D.S., Lazzari, E., Benvenutti, E.V., Falcade, T., Jacques, R.A., 2020. Activated carbon from rice husk biochar with high surface area. Biointerface Res Appl. Chem. 11, 10265–10277. https://doi.org/10.33263/BRIAC113.1026510277.
Selvarajoo, A., Oochit, D., 2020. Effect of pyrolysis temperature on product yields of palm fibre and its biochar characteristics. Mater. Sci. Energy Technol. 3, 575–583. https://doi.org/10.1016/j.mset.2020.06.003.
Shahbaz, M., AlNouss, A., Parthasarathy, P., Abdelaal, A.H., Mackey, H., McKay, G., Al-Ansari, T., 2022. Investigation of biomass components on the slow pyrolysis products yield using Aspen Plus for techno-economic analysis. Biomass Convers. Biorefin 12, 669–681. https://doi.org/10.1007/s13399-020-01040-1.
Sunali, Mago, J., Negi, A., Pant, K.K., Fatima, S., 2022. Development of natural rubber-bamboo biochar composites for vibration and noise control applications. J. Clean. Prod. 373, 133760 https://doi.org/10.1016/j.jclepro.2022.133760.
Tengku Yasim-Anuar, T.A., Yee-Foong, L.N., Lawal, A.A., Ahmad Farid, M.A., Mohd Yusuf, M.Z., Hassan, M.A., Ariffin, H., 2022. Emerging application of biochar as a renewable and superior filler in polymer composites. RSC Adv. 12, 13938–13949. https://doi.org/10.1039/D2RA01897G.
Tripathi, M., Sahu, J.N., Ganesan, P., 2016. Effect of process parameters on production of biochar from biomass waste through pyrolysis: a review. Renew. Sustain. Energy Rev. 55, 467–481. https://doi.org/10.1016/j.rser.2015.10.122.
TSAI, W., LEE, M., CHANG, Y., 2007. Fast pyrolysis of rice husk: Product yields and compositions. Bioresour. Technol. 98, 22–28. https://doi.org/10.1016/j.biortech.2005.12.005.
Ulfah, I.M., Fidyaningsih, R., Rahayu, S., Fitriani, D.A., Saputra, D.A., Winarto, D.A., Wisojodharmo, L.A., 2015. Influence of carbon black and silica filler on the rheological and mechanical properties of natural rubber Compound. Procedia Chem. 16, 258–264. https://doi.org/10.1016/j.proche.2015.12.053.
Vaghela, D.R., Pawar, A., Sharma, D., 2023. Effectiveness of wheat straw biochar in aqueous Zn removal: correlation with biochar characteristics and optimization of process parameters. Bioenergy Res. 16, 457–471. https://doi.org/10.1007/s12155-022-10471-9.
Wang, G., Gao, M., Yang, B., Chen, Q., 2020. The morphological effect of carbon fibers on the thermal conductive composites. Int. J. Heat Mass Transf. 152, 119477 https://doi.org/10.1016/j.ijheatmasstransfer.2020.119477.
Yang, H., Yan, R., Chen, H., Lee, D.H., Zheng, C., 2007. Characteristics of hemicellulose, cellulose and lignin pyrolysis. Fuel 86, 1781–1788. https://doi.org/10.1016/j.fuel.2006.12.013.
Zhang, J., Liu, J., Liu, R., 2015. Effects of pyrolysis temperature and heating time on biochar obtained from the pyrolysis of straw and lignosulfonate. Bioresour. Technol. 176, 288–291. https://doi.org/10.1016/j.biortech.2014.11.011.
Zhang, Y., Sun, X., Bian, W., Peng, J., Wan, H., Zhao, J., 2020. The key role of persistent free radicals on the surface of hydrochar and pyrocarbon in the removal of heavy metal-organic combined pollutants. Bioresour. Technol. 318, 124046 https://doi.org/10.1016/j.biortech.2020.124046.
Zhang, Q., Zhang, D., Xu, H., Lu, W., Ren, X., Cai, H., Lei, H., Huo, E., Zhao, Y., Qian, M., Lin, X., Villota, E.M., Mateo, W., 2020. Biochar filled high-density polyethylene composites with excellent properties: towards maximizing the utilization of agricultural wastes. Ind. Crops Prod. 146, 112185 https://doi.org/10.1016/j.indcrop.2020.112185.
Zhang, X., Zhang, P., Yuan, X., Li, Y., Han, L., 2020. Effect of pyrolysis temperature and correlation analysis on the yield and physicochemical properties of crop residue

biochar. Bioresour. Technol. 296, 122318 https://doi.org/10.1016/j.biortech.2019.122318.
Zhao, W., He, J., Yu, P., Jiang, X., Zhang, L., 2023. Recent progress in the rubber antioxidants: a review. Polym. Degrad. Stab. 207, 110223 https://doi.org/10.1016/j.polymdegradstab.2022.110223.
Zhao, S.-X., Ta, N., Wang, X.-D., 2017. Effect of temperature on the structural and physicochemical properties of biochar with apple tree branches as feedstock material. Energies 10, 1293. https://doi.org/10.3390/en10091293.